Stochastic perturbations of the five-components Benard system

1984 J. Phys. A: Math. Gen. 17 2551

(http://iopscience.iop.org/0305-4470/17/12/025)

J. Phys. A: Math. Gen. 17 (1984) 2551–2565. Printed in Great Britain

Stochastic perturbations of the five-component Bénard system

Roberto Benzi† and Alfonso Sutera‡

† Centro Scientifico IBM, Via del Giorgione 129 Roma, Italy
‡ The Center for the Environment and Man, Windsor Street 275, 06120 Hartford, Connecticut, USA

Received 9 August 1983

Abstract. We study the effect of small stochastic perturbations on a simple dynamical system describing a Bénard flow.

1. Introduction

In this paper we study the effect of small stochastic perturbations on a severely truncated two-dimensional convective fluid system. There have been several papers that consider the same problem for the Lorenz model (Sutera 1980, Moritz and Sutera 1981, Zippelius and Lucke 1981). In these studies it has been noticed that the noise induces transition at random times among the stable steady states of the system. In this case, chaotic behaviour, similar to turbulence motion, would be generated by the effect of the noise. However a large noise is required if such transitions have to occur on a time scale of any possible physical interest.

We investigate the effect of introducing additional scales in the limit of large aspect ratio of the system. In particular we study how the transition time, i.e. the average exit time from the attraction basin of stable steady states, depends *on the additional scales and on the aspect ratio.* We find that for large value of the aspect ratio and particular choice of the additional scales the same noise that would produce very long exits in the Lorenz model, is able to trigger exits on a much shorter time scale. We believe that this effect is quite general for systems with large aspect ratios. This belief follows from a simple dimensional argument independent of our model. The dimensionless time variable in a Bénard system is

$$t_{ad} = (\nu / H^2)t$$

where H is the thickness of the layer. It follows that large aspect ratios ($H \to 0$, L fixed) correspond to an infinite dimensionless time scale in which the motion occurs. On the other hand, the dimensionless time scale of Wiener's process with variance ε is $1/\varepsilon$. Hence when $1/\varepsilon \sim \nu/H$ the effect of the noise occurs on the same time scale of the deterministic dynamics. Indeed we will show, with our simple model, that the statistical properties of the system depend of the quantity $\varepsilon\Gamma^2$ ($\Gamma = L/H$ aspect ratio). There is scarce evidence from laboratory experiments (Ahlers and Walden 1980, Greenside *et al* 1983) that a mechanism, similar to the one here discussed, occurs. However, if the previous scale argument is correct, this mechanism should be observed for a proper choice of the physical parameters. In this case, we propose a technique

0305-4470/84/122551+15$02.25

to detect if the noise is responsible for the transitions and to measure its variance. This technique is based upon the concept of stochastic resonance as discussed by Benzi *et al* (1981).

In § 2 we describe the model employed. Section 3 is devoted to the discussion of an asymptotic estimates of the exit integrations in § 4. In § 5 the mechanism of stochastic resonance is discussed for the model. Conclusions follow in § 6.

2. The model

The physical system we consider is a two-dimensional fluid layer heated from below with periodic free stress boundary conditions. Following Saltzman (1962), we write the equations of motion in a dimensionless form:

$$\begin{aligned} &\partial_t \Delta\psi + J(\psi, \Delta\psi) - \sigma\partial_x\Theta - \sigma\Delta^2\psi = 0 \\ &\partial_t\Theta + J(\psi, \Theta) - Ra\partial_x\psi - \Delta\Theta = 0 \end{aligned} \tag{1}$$

(a list of symbol is given in appendix 1). Using the periodic boundary conditions, we expand ψ and Θ in a Fourier series:

$$\begin{aligned} \psi(x, z, t) &= \sum_{ln} \psi(l, n, t) \exp\left[2\pi i H\left(\frac{l}{L}x + \frac{nz}{2H}\right)\right] \\ \Theta(x, z, t) &= \sum_{ln} \Theta(l, n, t) \exp\left[2\pi i H\left(\frac{l}{L}x + \frac{nz}{2H}\right)\right]. \end{aligned} \tag{2}$$

The system of partial differential equations (1) is an infinite system of ordinary differential equations for the modes $\psi(l, n, t)$ and $\Theta(l, n, t)$ (Saltzman 1962). Among all the modes, we select the five terms

$$\text{Re } \psi(m, 1), \text{ Im } \Theta(m, 1), \text{ Re } \psi(p, 1), \text{ Im } \Theta(p, 1). \text{ Im } \Theta(0, 2). \tag{3}$$

Physically they describe a system of two Rayleigh rolls, one with wavenumber m and the other one with wavenumber p, interacting through the temperature gradient Im $\Theta(0, 2)$. No inertial interaction of the velocity field is considered. According to Busse (1978), this implies certain limitations on both the Prandtl number and the boundary conditions. In this paper we will not investigate this point.

By using the following scaling

$$\begin{aligned} x_m &= S_m \text{ Re } \psi(m, 1) \qquad & x_p &= S_p \text{ Re } \psi(p, 1) \\ y_m &= T_m \text{ Im } \Theta(m, 1) \qquad & y_p &= T_p \text{ Im } \Theta(p, 1) \\ z &= T_2 \text{ Im } \Theta(0, 2) \end{aligned}$$

(S_m, S_p, T_m, T_p and T_2 are listed in appendix 1), we get a dynamical system which describes the deterministic evolution of the modes (3):

$$\dot{x}_m = \sigma(y_m - x_m) \tag{4a}$$

$$\dot{y}_m = rx_m - y_m - x_m z \tag{4b}$$

$$\dot{x} = \sigma(\alpha_p/\alpha_m)(y_p - x_p) \tag{4c}$$

$$\dot{y}_p = (\alpha_p/\alpha_m)[(r_m/r_p)rx_p - y_p - (r_m/r_p)zx_p] \tag{4d}$$

$$\dot{z} = -bz + x_m y_m + x_p y_p. \tag{4e}$$

When $x_p = y_p = 0$, (4*a*), (4*b*) and (4*e*) reduce to the Lorenz model.

The wavenumber m is chosen such that r_m is a minimum, which implies that m is the critical wavenumber (Busse 1978) and it depends on the aspect ratio $\Gamma = L/H$ through the relationship

$$m^2 = \tfrac{1}{8}\Gamma^2. \tag{5}$$

Using equation (5) we obtain $b = \frac{8}{3}$ in (4*e*); the same value used by Lorenz (1963). (5) implies $r_p > r_m$ for any p. Hereafter we choose $p = m + 1$ which minimises the ratio r_p/r_m. Leaving the Prandtl number as a free parameter, our model is completely specified.

We discuss the effect of stochastic perturbations on the dynamical system (4). We model an external stochastic perturbation by using an additive white noise:

$$\begin{aligned}
\mathrm{d}x_m &= \sigma(y_m - x_m)\,\mathrm{d}t + \varepsilon_1^{1/2}\,\mathrm{d}w_1 \\
\mathrm{d}y_m &= (rx_m - y_m - zx_m)\,\mathrm{d}t + \varepsilon_2^{1/2}\,\mathrm{d}w_2 \\
\mathrm{d}x_p &= \sigma(\alpha_p/\alpha_m)(y_p - x_p)\,\mathrm{d}t + \varepsilon_3^{1/2}\,\mathrm{d}w_3 \\
\mathrm{d}y_p &= \{(\alpha_p/\alpha_m)[(r_m/r_p)rx_p - y_p - (r_m/r_p)zx_p]\}\,\mathrm{d}t + \varepsilon_4^{1/2}\,\mathrm{d}w_4 \\
\mathrm{d}z &= (-bz + x_m y_m + x_p y_p)\,\mathrm{d}t + \varepsilon_5^{1/2}\,\mathrm{d}w_5
\end{aligned} \tag{6}$$

where $\mathrm{d}w_i$ are Wiener processes, $\langle \mathrm{d}w_i\,\mathrm{d}w_j \rangle = \delta_{ij}\,\mathrm{d}t$ and $\varepsilon_i \ll 1$ for $i = 1 \ldots 5$. From the theory of stochastic differential equations, we know that in the limit $\varepsilon_i \to 0$ the solution of the system (6) forms a Markov process, its states being the steady solutions and the periodic orbits of the deterministic system (4); transitions among the states happen at random times. Our goal is to estimate the average value of these times as a function of the aspect ratio, the Rayleigh number, the Prandtl number and ε_i.

3. Analytical results

We confine our analysis in the range of the Rayleigh number $1 < Ra/Ra_c \leqslant 2$ where Ra_c is the critical Rayleigh number. It implies that $1 < r \leqslant 2$. In this case no hydrodynamical instability of Rayleigh's rolls can occur for equations (1) (Busse 1978). As a consequence the phase space of the system is characterised only by stable and unstable fixed points. In table 1 we summarise the positions and the stability of the fixed points in our model. By the symmetry of the system, we need to compute only the average transition time between the two stable steady states P_1 and P_2.

Let us consider a system of stochastic differential equations

$$\mathrm{d}x_i = f_i(\mathbf{x})\,\mathrm{d}t + \varepsilon_i^{1/2}\,\mathrm{d}w_i \tag{7}$$

where $i = 1 \ldots N$. Let $P = (x_1, x_2, \ldots x_N)$ be a stable fixed point of the deterministic vector field f and Ω its basin of attraction:

$$f_i(\underline{x}) = 0.$$

The average exit time from Ω with initial conditions $x_i(0) = y_i$ is defined as

$$\tau(\mathbf{y}) = \inf\{t\colon x_i(t) \in \partial\Omega\,;\, x_i(0) = y_i\}$$

Table 1. Fixed points and their stability properties for the deterministic equations (4).

Fixed points						Stability properties
	x_m,	y_m,	x_p,	y_p,	z	
P_1 =	$(-D$,	$-D$,	0,	0,	$G)$	stable for $1 < r < r_T$
P_2 =	$(+D$,	$+D$,	0,	0,	$G)$	stable for $1 < r < r_T$
P_3 =	(0,	0,	$-F$,	$-F$,	$H)$	unstable
P_4 =	(0,	0,	$+F$,	$+F$,	$H)$	unstable
P_5 =	(0,	0,	0,	0,	0)	stable for $r < 1$, unstable for $r > 1$.

$D = [b(r-1)]^{1/2}$, $F = [b(r - r_p/r_m)]^{1/2}$, $G = r - 1$, $H = r - r_p/r_m$, $r_T = \sigma(\sigma + b + 3)/(\sigma - b - 1)$.

where $\partial\Omega$ is the boundary of Ω. $\tau(y)$ is the solution of Dynkin's equation (Dynkin 1965):

$$\sum_i \left[\tfrac{1}{2}\varepsilon_i \frac{\partial^2 \tau}{\partial y_i^2} + f_i \frac{\partial \tau}{\partial y_i} \right] = -1 \tag{8}$$

with boundary conditions $\tau(y) = 0$ for $y_i \in \partial\Omega$. If f_i is the gradient of a function ϕ, then an estimation for $\tau(y)$ can be found using the saddle-point technique to evaluate the solution of equation (8). In this section we shall use this fact to estimate the average exit time for the system of stochastic differential equations (6).

In order to reduce the deterministic part of (6) to the gradient of a function, we employ asymptotic methods for stochastic differential equations (Papanicolau 1978, Graham and Schenlze 1983). These methods can be applied on (6) using different techniques sharing the common assumption that the deterministic dissipative times are much shorter than any other time scale of the system. In our case, the assumption is equivalent to considering $(r-1)$ small enough such that the probability distribution can be approximated as power series of the 'small' parameters $1/b$ and $1/(\sigma+1)$. The expansion can be carried out by using the system of stochastic differential equations (6) which, to the first order in $1/b$ and $1/(\sigma+1)$, reduces to the following for (see appendix 2 for details)

$$\begin{aligned} \mathrm{d}x_m = {} & \frac{\sigma}{\sigma+1}\left[\left(r - 1 + \frac{\varepsilon_1}{\sigma} + \frac{\alpha_m}{\sigma\alpha_p}\varepsilon_3\right)x_m - \frac{x_m^3}{b} - \frac{x_m x_p^2}{b}\right]\mathrm{d}t \\ & + \varepsilon_1^{1/2}\left(1 - \frac{\sigma}{\sigma+1} + \frac{x_m^2}{\sigma+1}\right)\mathrm{d}\omega_1 + \varepsilon_2^{1/2}\frac{\sigma}{\sigma+1}\mathrm{d}w_2 + \varepsilon_3^{1/2}\frac{\alpha_m}{\alpha_p(\sigma+1)}x_m x_p\,\mathrm{d}w_3 \\ & - \varepsilon_5^{1/2}\frac{\sigma}{\sigma+1}x_m\,\mathrm{d}w_5 \end{aligned} \tag{9}$$

$$\begin{aligned} \mathrm{d}x_p = {} & \frac{\sigma}{\sigma+1}\left[\frac{\alpha_p}{\alpha_m}\left(\frac{r_m}{r_p}r - 1 + \frac{\varepsilon_1}{\sigma} + \frac{\alpha_m\varepsilon_3}{\sigma\alpha_p}\right)x_p - \frac{r_m}{br_p}x_p x_m^2 - \frac{r_m}{r_p b}x_p^3\right]\mathrm{d}t \\ & + \frac{\alpha_p r_m}{\alpha_m r_p(\sigma+1)}\varepsilon_1^{1/2}x_p x_m\,\mathrm{d}w_1 + \varepsilon_3^{1/2}\left[1 - \frac{\sigma}{\sigma+1} + \frac{\sigma r_m x_p^2}{r_p(\sigma+1)}\right]\mathrm{d}w_3 \\ & + \varepsilon_4^{1/2}\frac{\sigma}{\sigma+1}\mathrm{d}w_4 - \varepsilon_5^{1/2}\frac{\sigma r_m\alpha_p}{\alpha_m r_p(\sigma+1)}x_p\,\mathrm{d}w_5. \end{aligned}$$

The deterministic forcing on the right-hand side of (9) depends on ε_1 and ε_3, due to

Ito's calculus applied in appendix 2. The overall effect of these terms is to renormalise the critical value of r at which finite amplitude convection develops. For small values of ε_1 and ε_3 we can neglect these terms. We also disregard all the terms on the right-hand side of equations (9) containing products of x_m and x_p with Wiener's processes. Again the latest approximation is valid in the limit of very small noises.

Introducing the variables

$$A_m = x_m(r_m/\alpha_m)^{1/2} \tag{10}$$

$$A_p = x_p(r_p/\alpha_p)^{1/2} \tag{11}$$

$$\varepsilon = \min\left\{\varepsilon_1\left(1-\frac{\sigma}{\sigma+1}\right)^2+\varepsilon_2\left(\frac{\sigma}{\sigma+1}\right)^2;\left(\frac{r_p\alpha_m}{r_m\alpha_p}\right)^{1/2}\left[\varepsilon_3\left(1-\frac{\sigma}{\sigma+1}\right)^2+\varepsilon_4\left(\frac{\sigma}{\sigma+1}\right)^2\right]\right\}, \tag{12}$$

we finally obtain

$$\begin{aligned} \mathrm{d}A_m &= \frac{\sigma}{\sigma+1}\left((r-1)A_m-\frac{\alpha_m^2}{4\pi^2 r_m}A_m^3-\frac{\alpha_p\alpha_m}{4\pi^2 r_p}A_mA_p^2\right)\mathrm{d}t+\varepsilon^{1/2}\left(\frac{r_m}{\alpha_m}\right)^{1/2}\mathrm{d}w_m \\ \mathrm{d}A_p &= \frac{\sigma}{\sigma+1}\left[\frac{\alpha_p}{\alpha_m}\left(\frac{r_m}{r_p}r-1\right)A_p-\frac{\alpha_m\alpha_p}{4\pi^2 r_p^2}A_pA_m^2-A_p^3\frac{\alpha_p^2 r_m}{4\pi^2 r_p^2}\right]\mathrm{d}t+\varepsilon^{1/2}\left(\frac{r_m}{\alpha_m}\right)^{1/2}\mathrm{d}w_p. \end{aligned} \tag{13}$$

We remark that because of the several approximations employed here, the estimate for the average exit time for (13) is only an upper bound of the average exit time for (6). This upper bound should be close to the true values in the limit of small variance of the noise.

The change of variables (10) and (11) have been determined in a way such that the deterministic vector field of (13) is the gradient of the function ϕ

$$\begin{aligned} \phi = \frac{\sigma}{\sigma+1}\Bigg[&\frac{\alpha_m^2}{16\pi^2 r_m}A_m^4+\frac{r_m}{r_p}\frac{\alpha_p^2A_p^4}{16\pi^2 r_p}-\tfrac{1}{2}(r-1)A_m^2 \\ &-\frac{1}{2}\frac{\alpha_p}{\alpha_m}\left(\frac{r_m}{r_p}r-1\right)A_p^2+\frac{1}{8}\frac{\alpha_m\alpha_p}{r_p\pi^2}A_m^2A_p^2\Bigg]. \end{aligned} \tag{14}$$

Labelling the fixed points of (13) as in table 1, we easily compute the average exit times from the basin of attraction of P_1 (see Schuss 1980):

$$\tau = A\exp(2/\varepsilon)(\alpha_m/r_m)\Delta\phi. \tag{15}$$

In equation (15) $\Delta\phi = \min\{|\phi(P_3)-\phi(P_1)|, |\phi(P_4)-\phi(P_1)|, |\phi(P_5)-\phi(P_1)|\}$ and A is a constant independent of ε, computed below. Because of the symmetry $\phi(P_3)=\phi(P_4)$. It follows that $\Delta\phi = \min\{|\phi(P_3)-\phi(P_1)|, |\phi(P_5)-\phi(P_1)|\}$.

We remark that in the Lorenz model (obtained from (4) for $x_p = y_p = 0$) the only fixed points are P_1, P_2 and P_5. It follows that the exit time for the Lorenz model is given by equation (15) with $\Delta\phi = \{|\phi(P_5)-\phi(P_4)|\}$. Thus the effect of Rayleigh's roll described by modes x_p and y_p is summarised as follows: if $\phi(P_3)<\phi(P_5)$ then the average exit time from the basin of attraction of P_1 is smaller than the corresponding average exit time for the Lorenz model. In this case, the interaction between the two Rayleigh rolls enhances the probability of transition between the stable steady states of the system. By straightforward algebraic calculations, we obtain

$$\phi(P_3)-\phi(P_1) = \frac{\sigma}{\sigma+1}\frac{r_m\pi^2}{\alpha_m^2}\left[2r\left(1-\frac{r_p}{r_m}\right)-\left(1-\frac{r_p^2}{r_m^2}\right)\right] \tag{16}$$

$$\phi(P_5)-\phi(P_1)=\frac{\sigma}{\sigma+1}\pi^2\frac{r_m}{\alpha_m^2}(r-1)^2. \tag{17}$$

It is easy to show that $\phi(P_3)<\phi(P_5)$ for $r>1$ and for any value of Γ and σ.

Using the ray method, as discussed in Schuss (1980) and Ludwig (1975), it is possible to compute the constant A in equations (15). The final result for the average exit time is

$$\tau=\frac{\pi(\sigma+1)}{2\sigma[(r_p/r_m)-1]}\left(\frac{r(r_m/r_p)-1}{r-1}\right)^{1/2}\exp\frac{2\sigma\pi^2}{\varepsilon(\sigma+1)\alpha_m}(1-r_p/r_m)(2r-1-r_p/r_m). \tag{18}$$

In the limit of large aspect ratio, we can evaluate τ from (18) as a power series of $1/\Gamma$. Recalling that $m^2=\frac{1}{8}\Gamma^2$ and $p=m+1$ we obtain

$$\tau=\frac{\pi}{2}\frac{\sigma+1}{\sigma}\frac{3\Gamma^2}{32}\exp\frac{8\sigma}{3\varepsilon(\sigma+1)}(r-1)\frac{32}{3\Gamma^2}. \tag{19}$$

Equation (19) requires two remarks. First, for $\Gamma\to\infty$ and fixed value of ε, (19) looses its validity because the saddle-point technique is no longer a good approximation. In this case solutions of (6) are similar to a random walk on the trajectory linking the points $P_1-P_3-P_2-P_4$ with diffusion time proportional to $1/\varepsilon$. Secondly the exponential dependence of τ on Γ^2 implies that the effect of stochastic forcing is amplified by a factor Γ^2. In clarifying this effect, we calculate the average exit time in the case of Lorenz model. This is done using equations (13) with $A_p=0$:

$$\mathrm{d}A_m=\frac{\sigma}{\sigma+1}\left((r-1)A_m-\frac{1}{b}A_m^3\right)\mathrm{d}t+\varepsilon^{1/2}\left(\frac{r_m}{\alpha_m}\right)^{1/2}\mathrm{d}w_m. \tag{20}$$

In the limit of large Γ, we obtain

$$\tau_{\text{Lorenz}}=\frac{\pi(\sigma+1)}{\sqrt{2}\sigma(r-1)}\exp\frac{4}{3\varepsilon}\frac{\sigma}{\sigma+1}(r-1)^2. \tag{21}$$

Thus for instance, for $\Gamma=20$ and $\varepsilon=0.01$, $r=2$ and $\sigma=1$ from (19) we obtain

$$\tau=4124$$

while for the Lorenz model we have

$$\tau_{\text{Lorenz}}\cong 3.57\times 10^{58}.$$

4. Numerical results

To test the performance of approximation (19), two sets of numerical integrations have been done: one for fixed noise and different aspect ratios and the other for increasing noise with smaller aspect ratios. In both cases we set $\sigma=1$. In the first set of numerical integrations the value of ε, was 0.02 and the values of the aspect ratios were $6\sqrt{2}$, $8\sqrt{2}$, $10\sqrt{2}$, $12\sqrt{2}$ and $14\sqrt{2}$. Figure 1 shows $x_m(t)$ as a function of time for the different aspect ratios. The behaviour of the system agrees with the discussion given at the end of the previous section: larger aspect ratios correspond to stronger effects of the noise in the system.

In table 2 a quantitative comparison between numerical integrations and equations (19) is given. The number of exits in the samples are compared with the theoretical

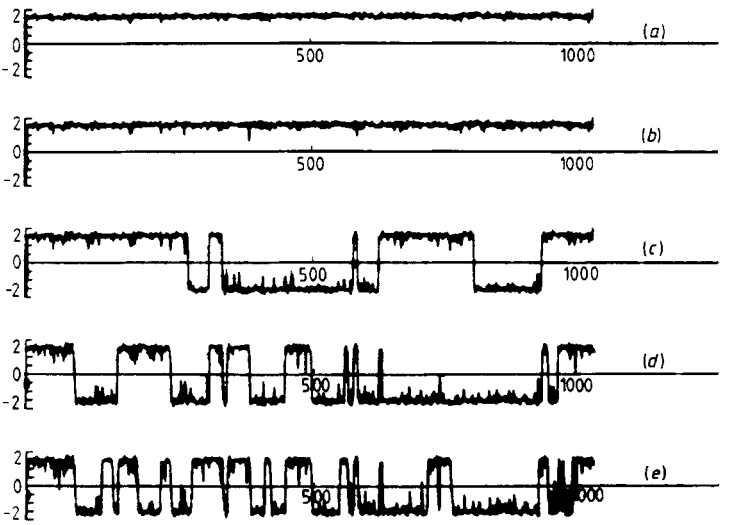

Figure 1. x_m as function of time for increasing aspect ratios, (*a*) $6\sqrt{2}$, (*b*) $8\sqrt{2}$, (*c*) $10\sqrt{2}$, (*d*) $12\sqrt{2}$ and (*e*) $14\sqrt{2}$. The parameter values are $\varepsilon_i = 0.02$, $\sigma = 1$, $r = 2$. The display time is 120 time units of the model.

Table 2. Theoretical and computed numbers of exits for the numerical integrations of figure 1. The value of Γ is given by $2m\sqrt{2}$. The theoretical estimates are obtained using equation (19).

m	Observed exits	Predicted exits
3	0	0
4	0	0
5	8	3
6	18	15
7	36	35

prediction. The estimates obtained using (19) agree fairly well with the numerical results, the agreement being better for larger aspect ratios.

For a more quantitative verification, we performed a second numerical test using different noises with different aspect ratios. The noise has been chosen such that the theoretical estimate for the exit time is constant. This gives a relationship between the noise and the aspect ratio:

$$\varepsilon = \frac{8\sigma(r-1)}{3(\sigma+1)} \frac{32}{3\Gamma^2} \ln\left(\frac{\pi(\sigma+1)}{2\tau\sigma} \frac{3\Gamma^2}{32}\right). \tag{22}$$

We choose τ to be 3411 corresponding to $\Gamma = 14\sqrt{2}$ and $\varepsilon_i = 0.02$. In figure 2 x_m is plotted aainst time, while figure 3 reports x_m for the same numerical integration keeping $x = y = 0$ (i.e. for the Lorenz model). The number of exits is a smooth function of the aspect ratio which confirms the validity of (19). Moreover the theory agrees in estimating the amplification of the noise with respect to the Lorenz model. Indeed in figure 3 no exits are shown for the stochastically perturbed Lorenz model, although the same noise has been used. Figure 4 is the projection of the numerical solution into the plane x_m,

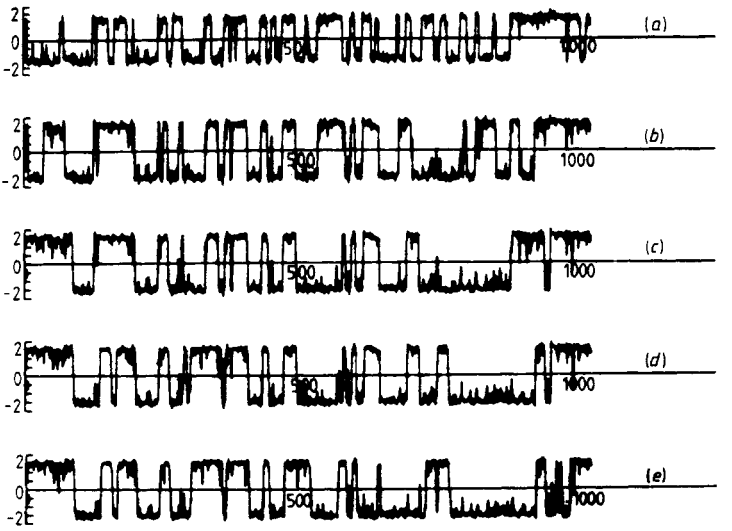

Figure 2. As figure 1 for increasing values of the noise. The values of ε_i are obtained, using equation (19), such that the average exit time is independent of Γ.

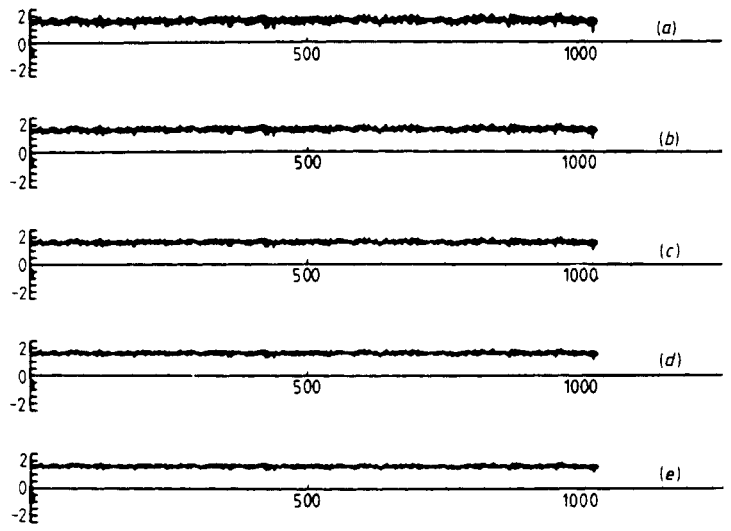

Figure 3. As in figure 2 for the case $x_p = y_p = 0$ (the Lorenz model).

x_p for $\Gamma = 14\sqrt{2}$. We see that the path of exits are trajectories passing through the unstable fixed points P_3, P_4.

We conclude that (19) can be used with good accuracy in calculating the statistical properties of the stochastic differential equations (6).

5. The stochastic resonance

The mechanism of stochastic resonance has been discussed by Benzi *et al* (1981 hereafter

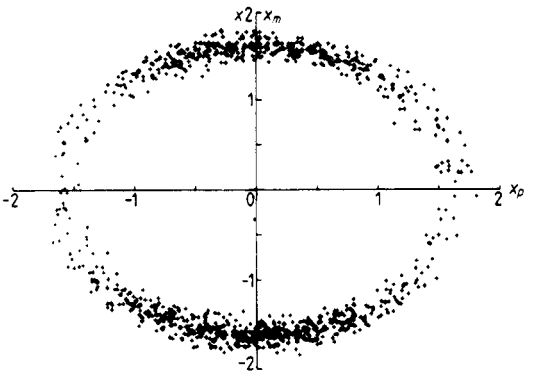

Figure 4. Phase space x_m, x_p for $\Gamma = 14\sqrt{2}$, $\varepsilon_1 = 0.02$, $\sigma = 1$ and $r = 2$ (case (*e*) of figure 1).

referred to as I) in the case of stochastic differential equation

$$\mathrm{d}x = [x(a - x^2) + A\cos\omega t]\,\mathrm{d}t + \varepsilon^{1/2}\,\mathrm{d}w. \tag{23}$$

In I it was shown that the solution of (23) has nearly periodic transitions between the two stable fixed points ($\pm\sqrt{a}$) when the following two conditions are satisfied

$$\text{(a)} \qquad \frac{\pi}{a\sqrt{2}}\exp\frac{a^2}{2\varepsilon}\left(1 - \frac{4A}{a^{3/2}}\right) \gg \frac{\pi}{\omega}$$

$$\text{(b)} \qquad \frac{\pi}{a\sqrt{2}}\exp\frac{a^2}{2\varepsilon}\left(1 + \frac{4A}{a^{3/2}}\right) \ll \frac{\pi}{\omega}.$$

We discuss this mechanism in the framework of the system defined by (6). We introduce a slow periodic forcing term on the right-hand side of (6*b*):

$$\begin{aligned}
\mathrm{d}x_m &= \sigma(y_m - x_m)\,\mathrm{d}t + \varepsilon_1^{1/2}\,\mathrm{d}w_1 \\
\mathrm{d}y_m &= [rx_m - y_m - x_m z + B\cos\omega t]\,\mathrm{d}t + \varepsilon_2^{1/2}\,\mathrm{d}w_2 \\
\mathrm{d}x_p &= \sigma(\alpha_p/\alpha_m)(y_p - x_p)\,\mathrm{d}t + \varepsilon_3^{1/2}\,\mathrm{d}w_3 \\
\mathrm{d}y_p &= \left(\frac{\alpha_p}{\alpha_m}[(r_m/r_p)rx_p - y_p - (r_m/r_p)zx_p]\right)\mathrm{d}t + \varepsilon_4^{1/2}\,\mathrm{d}w_4 \\
\mathrm{d}z &= (-bz + x_m y_m + x_p y_p)\,\mathrm{d}t + \varepsilon_5^{1/2}\,\mathrm{d}w_5.
\end{aligned} \tag{24}$$

Performing the same asymptotic analysis as that discussed in § 3 and in appendix 2, we derive the set of two stochastic differential equations

$$\begin{aligned}
\mathrm{d}A_m = \frac{\sigma}{\sigma+1}\Bigg[&(r-1)A_m - \frac{\alpha_m^2}{4\pi^2 r_m}A_m^3 - \frac{\alpha_m\alpha_p}{4\pi^2 r_p}A_m A_p^2 + \left(\frac{r_m}{\alpha_m}\right)^{1/2} B\cos\omega t\Bigg]\mathrm{d}t \\
&+ \varepsilon^{1/2}\left(\frac{r_m}{\alpha_m}\right)^{1/2}\mathrm{d}w_m
\end{aligned} \tag{25}$$

$$\mathrm{d}A_p = \frac{\sigma}{\sigma+1}\left[\frac{\alpha_p}{\alpha_m}\left(\frac{r_m}{r_p}r - 1\right)A_p - \frac{\alpha_m\alpha_p}{4\pi^2 r_p^2}A_p A_m^2 - A_p^3\frac{\alpha_p^2 r_m}{4\pi^2 r_p^2}\right]\mathrm{d}t + \varepsilon^{1/2}\left(\frac{r_m}{\alpha_m}\right)^{1/2}\mathrm{d}w_p$$

where A_m, A_p and ε have the same meaning as in § 3. To study the effect of the

periodic forcing in (25) we follow the theory given in I. The solution of (25) shows nearly periodic transition when the following conditions are satisfied

$$\text{(i)} \qquad \frac{\pi(\sigma+1)}{2\sigma[(r_p/r_m)-1]}\left(\frac{r(r_m/r_p)-1}{r-1}\right)^{1/2}\exp\frac{2\sigma\pi^2}{\varepsilon\alpha_m(\sigma+1)}\left(1-\frac{r_p}{r_m}\right)\left(2r-1-\frac{r_p}{r_m}\right)$$

$$\times(1-\Delta)\ll\frac{\pi}{\omega}$$

$$\text{(ii)} \qquad \frac{\pi(\sigma+1)}{2\sigma[(r_p/r_m)-1]}\left(\frac{r(r_m/r_p)-1}{r-1}\right)^{1/2}\exp\frac{2\sigma\pi^2}{\varepsilon\alpha_m(\sigma+1)}\left(1-\frac{r_p}{r_m}\right)\left(2r-1-\frac{r_p}{r_m}\right)$$

$$\times(1+\Delta)\gg\frac{\pi}{\omega}$$

where

$$\Delta=\frac{2B\alpha_m[\pi^2(r-1)/\alpha_m]^{1/2}}{\pi^2(1-r_p/r_m)(2r-1-r_p/r_m)}.$$

(i) and (ii) are the analogues of (a) and (b) for (23).

We studied numerically the validity of (i) and (ii) choosing $\varepsilon_i = 0.02$, $\omega = 2\pi/7040$ and $B = 0.013\,56$. We performed numerical integrations for aspect ratios $6\sqrt{2}$, $8\sqrt{2}$, $10\sqrt{2}$, $12\sqrt{2}$ and $14\sqrt{2}$, as in § 4, with fixed values of ε, B and ω. These values satisfy conditions (i) and (ii) for $\Gamma = 12\sqrt{2}$ and $\Gamma = 14\sqrt{2}$. The values of Δ are 0.5 and 0.67 respectively. In figure 5 we plot x_m against time for the five aspect ratios. This figure has to be compared with figure 1 where the same noise and aspect ratios have been used without a periodic forcing. For $\Gamma = 12\sqrt{2}$ and $\Gamma = 14\sqrt{2}$ we observe almost periodic transitions between the two stable steady states.

Recalling that (i) and (ii) are obtained using the asymptotic expansion of § 3, the numerical test, performed here, is a further verification of the estimate (18) and (19) for the average exit times.

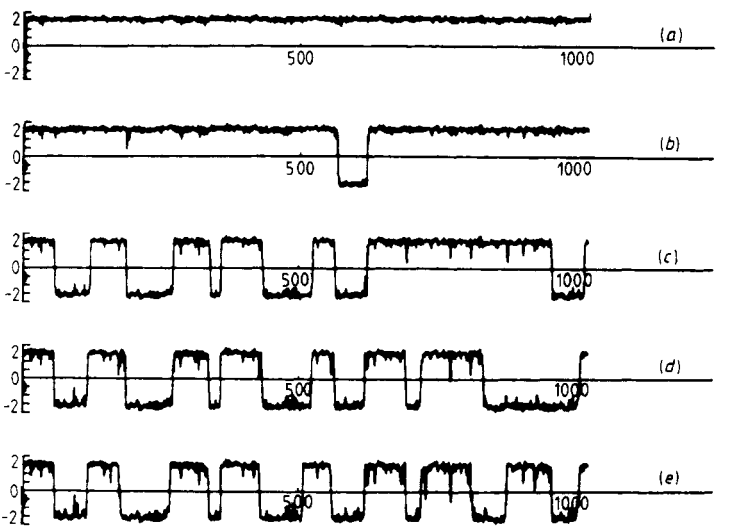

Figure 5. x_m as a function of time for equations (24). The parameter values are the same as in figure 1 and $B = 0.013\,56$.

As discussed in § 1, it has been observed (Ahlers and Walden 1980, Libchaber 1983) that for large aspect ratios the instability sequences which lead to chaotic behaviour are characterised by random transitions between two convective structure. Within the model described in this paper, we found that for large aspect ratios the effect of any stochastic perturbations is amplified by a factor proportional to Γ^2. The mechanism of stochastic resonance could be useful in detecting the dynamical features of the system by applying to it a periodic forcing with amplitude and period given as a function of the noise. An experimental test based on this idea might provide the way to measure the value of the noise acting in the system and to test the pattern of the convective structures characterising the system.

6. Conclusion

In this paper we have discussed the effect of stochastic perturbations in a particular model of a two-dimensional convective fluid. Our model can be regarded as the simplest generalisation of the Lorenz model with explicit dependence on the aspect ratio of the system. The statistical properties of the model have been studied for value of r in the range $[1, 2]$ by using the reduced system (13). We have verified that our asymptotic approximations agree with the numerical integrations.

Recently Knobloch and Guckenheimer (1983) have discussed a similar model in connection with the deterministic behaviour of the Bénard system with large aspect ratios. Using projection on the centre manifold, they found that for small values of the bifurcating parameter (namely r) a dynamical system of nine modes can be reduced to the amplitude equations for x_m and x_p considered in this paper. These amplitudes completely describe the behaviour of the system on the centre manifold. In view of this result we can argue that, for large aspect ratios, the validity of our analysis is independent of the choice of modes (4). If more degrees of freedom were considered, they would be deterministically damped on the centre manifold. In Benzi and Sutera (1983), projection on the central manifold was employed in the case of the stochastically perturbed Lorenz model. We found that the Landau equation on the centre manifold is similar to (20).

Summarising our results, we have seen that a Bénard system with large aspect ratio amplifies the effect of any external or internal stochastic perturbations acting on the system. This amplification causes transitions between the two competing convective rolls with wavenumber m (the critical wavenumber) and $p = m + 1$. We offer the speculation that the observed random behaviour for large aspect ratios (Ahlers and Walden 1980, Libchaber1983) might be induced by a mechanism similar to the one discussed in this paper. If this is the case, the mechanism of stochastic resonance discussed in § 5 will be useful in laboratory studies for detecting whether the structure of the convective flow is similar to the one considered here.

Acknowledgments

We are grateful to Professor A Libchaber for useful discussions. This work was done while one of us (AS) was supported by National Science Foundation Grant-ATM-8022869 at the Center for the Environment and Man, Inc.

Appendix 1

$\alpha_m = \pi^2(4m^2/\Gamma^2 + 1)$
$\alpha_p = \pi^2(4p^2/\Gamma^2 + 1)$
$b = 4\pi^2/\alpha_m$
$\Gamma = L/H$
H = height of the layer
L = width of the layer
ψ = dimensionless stream function
$r_m = 3\alpha_m^3\Gamma/2m^2\pi$
$r_p = 3\alpha_p^3\Gamma/2p^2\pi$
Ra = Rayleigh number
$S_m = 4\pi^2 m(2/\Gamma)^{1/2}/\alpha_m$
$S_p = 12\pi^2\alpha_p^2(1/6\alpha_m\pi r_m)^{1/2}$
$\sigma = \nu/k$ Prandtl number
$T_m = -12\pi^2(2/\Gamma)^{1/2}/r_m$
$T_p = -12\pi^2(2\alpha_p/\Gamma r_m r_p \alpha_m)^{1/2}$
$T_2 = 12\pi^2/\Gamma r_m$
Θ = dimensionless temperature departure from the convective state
x = horizontal coordinate
z = vertical coordinate.

Appendix 2

In this appendix we derive equations (12) from the set of stochastic differential equations (6) using the Smolukowsky–Kramers approximation as reviewed by Schuss (1980). Introducing the variables

$$\eta_m = \sigma(y_m - x_m)$$
$$\eta_p = \sigma(\alpha_p/\alpha_m)(y_p - x_p)$$
$$q = z - (x_m^2/2\sigma) - \alpha_m x_p^2/2\sigma\alpha_p,$$

the system of stochastic differential equations (6) transforms to

$$\mathrm{d}x_m = \eta_m\,\mathrm{d}t + \varepsilon_1^{1/2}\,\mathrm{d}w_1 \tag{A2.1a}$$

$$\mathrm{d}\eta_m = [-(\sigma+1)\eta_m + \sigma(r-1)x_m - \sigma q x_m - \tfrac{1}{2}x_m^3 - x_p^2 x_m/2\alpha]\,\mathrm{d}t + \sigma\varepsilon_2^{1/2}\,\mathrm{d}w_2 - \sigma\varepsilon_1^{1/2}\,\mathrm{d}w_1 \tag{A2.1b}$$

$$\mathrm{d}x_p = \eta_p\,\mathrm{d}t + \varepsilon_3^{1/2}\,\mathrm{d}w_3 \tag{A2.1c}$$

$$\mathrm{d}\eta_p = [-\alpha(\sigma+1)\eta_p + \alpha^2\sigma(Rr-1)x_p - \sigma\alpha^2 R q x_p - \tfrac{1}{2}\alpha R x_m^2 x_p - \tfrac{1}{2}\alpha R x_p^3]\,\mathrm{d}t + \sigma\alpha\varepsilon_4^{1/2}\,\mathrm{d}w_4 - \sigma\alpha\varepsilon_3^{1/2}\,\mathrm{d}w_3 \tag{A2.1d}$$

$$\mathrm{d}q = [-bq + x_m^2(1 - b/2\sigma) + x_p^2(1 - b/2\sigma\alpha) - \varepsilon_1/\sigma - \varepsilon_3/\sigma\alpha]\,\mathrm{d}t + \varepsilon_5^{1/2}\,\mathrm{d}w_5 - \varepsilon_1^{1/2}(x_m/\sigma)\,\mathrm{d}w_1 - \varepsilon_3^{1/2}(x_p/\alpha\sigma)\,\mathrm{d}w_3 \tag{A2.1e}$$

where $\alpha = \alpha_p/\alpha_m$ and $R = r_m/r_p$. Introducing the slow time variable $s = \varepsilon t$, where

$\varepsilon = \inf(\varepsilon_i)$, and integrating formally equations (A2.1) we obtain

$$x_m(s) = \frac{1}{\varepsilon}\int_0^s e^{-(\sigma+1)\rho/\varepsilon}\int_0^\rho e^{(\sigma+1)\theta/\varepsilon} f_m(\theta)\,d\theta\,d\rho + \lambda_1^{1/2}\int_0^s dw_1(\rho)$$
$$+\frac{1}{\varepsilon}\int_0^s e^{-\rho(\sigma+1)/\varepsilon}\int_0^\rho e^{(\sigma+1)\theta/\varepsilon}[\sigma\lambda_2^{1/2}\,dw_2(\theta) - \sigma\lambda_1^{1/2}\,dw_1(\theta)]\,d\rho \qquad (A2.2)$$

$$x_p(s) = \frac{1}{\varepsilon}\int_0^s e^{-\alpha(\sigma+1)\rho/\varepsilon}\int_0^\rho e^{\alpha(\sigma+1)\theta/\varepsilon} f_p(\theta)\,d\theta\,d\rho + \lambda_3^{1/2}\int_0^s dw_3(\rho)$$
$$+\frac{1}{\varepsilon}\int_0^s e^{-\alpha\rho(\sigma+1)/\varepsilon}\int_0^\rho e^{\alpha(\sigma+1)\theta/\varepsilon}[\alpha\sigma\lambda_4^{1/2}\,dw_4(\theta) - \sigma\alpha\lambda_3^{1/2}\,dw_3(\theta)]\,d\rho \qquad (A2.3)$$

$$q(s) = \frac{1}{\varepsilon}e^{-bs/\varepsilon}\int_0^s e^{b\rho/\varepsilon}\left[x_m^2(\rho)\left(1-\frac{b}{2\sigma}\right) + x_p^2(\rho)\left(1-\frac{b}{2\sigma\alpha}\right) - \frac{\varepsilon_1}{\sigma} - \frac{\varepsilon_2}{\sigma\alpha}\right]d\rho$$
$$+\lambda_5^{1/2}e^{-bs/\varepsilon}\int_0^s e^{b\rho/\varepsilon}\,dw_5(\rho) - \lambda_1^{1/2}e^{-b\rho/\varepsilon}\int_0^s e^{b\rho/\varepsilon}\frac{x_m(\rho)\,dw_1(\rho)}{\sigma}$$
$$-\lambda_3^{1/2}e^{-bs/\varepsilon}\int_0^s e^{b\rho/\varepsilon}\frac{x_p(\rho)}{\sigma\alpha}\,dw_3(\rho) \qquad (A2.4)$$

where

$$\lambda_i = \varepsilon_i/\varepsilon$$
$$f_m(\theta) = \sigma(r-1)x_m(\theta) - \sigma x_m(\theta)q(\theta) - \tfrac{1}{2}x_m^3(\theta) - (1/2\alpha)x_p^2(\theta)x_m(\theta)$$
$$f_p(\theta) = \sigma\alpha^2(Rr-1)x_p(\theta) - \sigma\alpha^2 R x_p(\theta)q(\theta) - \tfrac{1}{2}\alpha R x_m^2(\theta)x_p(\theta) - \tfrac{1}{2}\alpha R x_p^3(\theta).$$

In equations (A2.2), (A2.3) and (A2.4) we now use the approximations

$$[(\sigma+1)/\varepsilon]\exp -[(\sigma+1)/\varepsilon](\rho-\theta) \to \delta(\rho-\theta)$$
$$(b/\varepsilon)\exp -(b/\varepsilon)(\rho-\theta) \to \delta(\rho-\theta) \qquad (A2.5)$$

which are good approximations in the limit $(\sigma+1)/\varepsilon \to \infty$ and $b/\varepsilon \to \infty$ i.e. in the limit of small noises. Substituting (A2.4) into (A2.2) and (A2.3) and using approximations (A2.5) we obtain after a long but straightforward calculations:

$$x_m(s) = \frac{1}{\varepsilon(\sigma+1)}\int_0^s\left[\sigma\left(r-1+\frac{\varepsilon_1}{\sigma}+\frac{\varepsilon_3}{\sigma\alpha}\right)x_m(\rho) - \frac{x_m^3(\rho)}{b} - \frac{x_m(\rho)x_p^2(\rho)}{b}\right]d\rho$$
$$+\lambda_1^{1/2}\int_0^s dw_1(\rho) + \frac{\sigma}{\sigma+1}\int_0^s[\lambda_2^{1/2}\,dw_2(\rho) - \lambda_1^{1/2}\,dw_1(\rho)]$$
$$-\frac{\sigma}{\sigma+1}\int_0^s x_m(\rho)\lambda_5^{1/2}\,dw_5(\rho) + \frac{\lambda_1^{1/2}}{b(\sigma+1)}\int_0^s x_m^2(\rho)\,dw_1(\rho)$$
$$+\frac{\sigma\lambda_3^{1/2}}{\sigma+1}\int_0^s\frac{x_p(\rho)x_m(\rho)}{\sigma\alpha}\,dw_3(\rho) \qquad (A2.6)$$

$$x_p(s)=\frac{1}{\varepsilon(\sigma+1)\alpha}\int_0^s\left[\left(Rr-1+\frac{\varepsilon}{\sigma}+\frac{\varepsilon_3}{\sigma\alpha}\right)\sigma\alpha^2x_p(\rho)-\frac{R}{b}x_p(\rho)x_m^2(\rho)-\frac{R}{b}x_p^3(\rho)\right]\mathrm{d}\rho$$
$$+\lambda_3^{1/2}\int_0^s \mathrm{d}w_3(\rho)+\frac{\sigma}{\sigma+1}\int_0^s\left[\lambda_4^{1/2}\,\mathrm{d}w_q(\rho)-\lambda_3^{1/2}\,\mathrm{d}w_3(\rho)\right]$$
$$-\frac{\sigma\alpha R}{\sigma+1}\int_0^s x_p(\rho)\left(\lambda_5^{1/2}\,\mathrm{d}w_5(\rho)-\frac{\lambda_1^{1/2}}{\sigma}x_m(\rho)\,\mathrm{d}w_1(\rho)-\frac{\lambda_3^{1/2}x_p(\rho)}{\sigma\alpha}\,dw_3(\rho)\right) \tag{A2.7}$$

(A2.6) and (A2.7) are equivalent to the set of stochastic differential equations:

$$\mathrm{d}x_m=\frac{1}{\varepsilon}\frac{\sigma}{\sigma+1}\left[\left(r-1+\frac{\varepsilon_1}{\sigma}+\frac{\varepsilon_3}{\sigma\alpha}\right)x_m-\frac{x_m^3}{b}-\frac{x_p^2x_m}{b}\right]\mathrm{d}s$$
$$+\lambda_1^{1/2}\left[1-\frac{\sigma}{\sigma+1}+\frac{x_m^2}{b(\sigma+1)}\right]\mathrm{d}w_1(s)+\lambda_2^{1/2}\frac{\sigma}{\sigma+1}\,\mathrm{d}w_2(s)$$
$$+\lambda_3^{1/2}\frac{1}{\alpha(\sigma+1)}x_mx_p\,\mathrm{d}w_3(s)-\lambda_5^{1/2}\frac{\sigma}{\sigma+1}x_m\,\mathrm{d}w_5(s) \tag{A2.8}$$

$$\mathrm{d}x_p=\frac{1}{\varepsilon}\frac{\sigma}{\sigma+1}\left[\alpha\left(Rr-1+\frac{\varepsilon_1}{\sigma}+\frac{\varepsilon_3}{\sigma\alpha}\right)x_p-\frac{R}{b}x_px_m^2-\frac{R}{b}x_p^3\right]\mathrm{d}s$$
$$+\frac{\alpha R\lambda_1^{1/2}}{\sigma+1}x_px_m\,\mathrm{d}w_1+\lambda_3^{1/2}\left(1-\frac{\sigma}{\sigma+1}-\frac{\sigma Rx_p^2}{\sigma+1}\right)\mathrm{d}w_3$$
$$+\lambda_4^{1/2}\frac{\sigma}{\sigma+1}\,\mathrm{d}w_4-\lambda_1^{1/2}\frac{\sigma R\alpha}{\sigma+1}x_p\,\mathrm{d}w_5. \tag{A2.9}$$

Returning to the original time variable t, we finally obtain

$$\mathrm{d}x_m=\frac{\sigma}{\sigma+1}\left[\left(r-1+\frac{\varepsilon_1}{\sigma}+\frac{\varepsilon_3}{\sigma\alpha}\right)x_m-\frac{x_m^3}{b}-\frac{x_p^2x_m}{b}\right]\mathrm{d}t$$
$$+\varepsilon_1^{1/2}\left(1-\frac{\sigma}{\sigma+1}+\frac{x_m^2}{\sigma+1}\right)\mathrm{d}w_1+\varepsilon_2^{1/2}\frac{\sigma}{\sigma+1}\,\mathrm{d}w_2$$
$$+\varepsilon_3^{1/2}\frac{x_mx_p}{\alpha(\sigma+1)}\,\mathrm{d}w_3-\varepsilon_5^{1/2}\frac{\sigma}{\sigma+1}x_m\,\mathrm{d}w_5 \tag{A2.10}$$

$$\mathrm{d}x_p=\frac{\sigma}{\sigma+1}\left[\alpha\left(Rr-1+\frac{\varepsilon_1}{\sigma}+\frac{\varepsilon_3}{\sigma\alpha}\right)x_p-\frac{R}{b}x_px_m^2-\frac{R}{b}x_p^3\right]\mathrm{d}t$$
$$+\frac{\alpha R}{\sigma+1}\varepsilon^{1/2}x_px_m\,\mathrm{d}w_1+\varepsilon_3^{1/2}\left(1-\frac{\sigma}{\sigma+1}+\frac{\sigma R}{\sigma+1}x_p^2\right)\mathrm{d}w_3$$
$$+\varepsilon_4^{1/2}\frac{\sigma}{\sigma+1}\,\mathrm{d}w_4-\varepsilon_5^{1/2}\frac{\sigma R\alpha}{\sigma+1}x_p\,\mathrm{d}w_5 \tag{A2.11}$$

which are the equations used in § 3.

It is interesting to observe that for $x_p=0$ (i.e. for the Lorenz model) equation (A2.10) reduces to the Landau equation which is known to hold for small value of the bifurcating parameter r. This result shows, in some sense, the consistency of our approach in calculating the statistical properties of equations (6) for small value of r and ε_i. Finally

let us remark that the change of variables used in this appendix is equivalent to putting equations (6) in the Arnold–Jordan form by which the computation of the centre manifold can be readily carried out (see Knobloch and Guckenheimer 1983). It turns out that the equations of the centre manifold are in the deterministic part of equations (A2.10) and (A2.11).

References

Ahlers G and Walden R W 1980 *J. Phys. Lett.* **44** 445
Benzi R and Sutera A 1983 *Report number 6513-4048, IBM Scientific Center, Rome*
Benzi R, Sutera A and Vulpiani A 1981 *J. Phys. A: Math. Gen.* **14** L453
Busse F H 1978 *Rep. Prog. Phys.* **41** 1930–67
Dynkin E B 1965 *Markov Processes* (Berlin: Springer)
Graham R and Schenlze A 1983 *Phys. Rev.* A **26** 1676–85
Greenside H S, Alhers G, Hohenberg P C and Walden R W 1983 *Physica* **5D** 322–34
Knobloc E and Guckenheimer J 1983 *Phys. Rev.* A **27** 1 408–17
Kramers H A 1940 *Physica* **7** 284–304
Landau L D and Lifshitz E M 1959 *Fluid Mechanics* (London: Pergamon)
Libchaber A 1983 Private communication
Lorenz E N 1963 *J. Atmos. Sci.* **20** 130–41
Ludwig D 1975 *SIAM Rev.* **17** 4605–40
Moritz R E and Sutera A 1981 *Adv. Geophys.* **23** 345–83
Papanicolau G C 1978 in *MAA Studies in Probability Theory* ed M Rosenblatt (Math. Assoc. America) N18 pp 111–79
Saltzman B 1962 *J. Atmos. Sci.* **19** 329–41
Schuss Z 1981 *SIAM Rev.* **22** 2119–55
Smoluchowsky M 1916 *Phys. Z.* **17** 557–85
Stuart J T 1960 *J. Fluid Mech.* **9** 353–70
Sutera A 1980 *J. Atmos. Sci.* **37** 245
Ventsel A D and Friedlin M I 1970 *Usp Mat. Nauk.* **25** 3–55
Watson J 1960 *J. Fluid Mech.* **9** 371–89
Zippelius A and Lucke M 1981 *J. Stat. Phys.* **24** 345